Human Molecular Genetics, 2012, Vol. 21, No. 6 **1203–1216**
doi:10.1093/hmg/ddr552
Advance Access published on November 24, 2011

Long-term memory deficits in Huntington's disease are associated with reduced CBP histone acetylase activity

A. Giralt[1,2,3,†], M. Puigdellívol[1,2,3,†], O. Carretón[1,2,3], P. Paoletti[1,2,3], J. Valero[3,4], A. Parra-Damas[3,4], C.A. Saura[3,4], J. Alberch[1,2,3] and S. Ginés[1,2,3,*]

[1]Departament de Biologia Cel.lular, Immunologia i Neurociències, Facultat de Medicina, Universitat de Barcelona, Barcelona, Spain, [2]Institut d'Investigacions Biomèdiques August Pi i Sunyer (IDIBAPS), [3]Centro de Investigación Biomédica en Red sobre Enfermedades Neurodegenerativas (CIBERNED) and [4]Institut de Neurociències, Departament de Bioquímica i Biologia Molecular, Universitat Autònoma de Barcelona, Barcelona, Spain

Received September 6, 2011; Revised October 28, 2011; Accepted November 20, 2011

Huntington's disease (HD) is an autosomal dominant progressive neurodegenerative disorder caused by an expanded CAG/polyglutamine repeat in the coding region of the *huntingtin* (*htt*) gene. Although HD is classically considered a motor disorder, there is now considerable evidence that early cognitive deficits appear in patients before the onset of motor disturbances. Here we demonstrate early impairment of long-term spatial and recognition memory in heterozygous HD knock-in mutant mice ($Hdh^{Q7/Q111}$), a genetically accurate HD mouse model. Cognitive deficits are associated with reduced hippocampal expression of CREB-binding protein (CBP) and diminished levels of histone H3 acetylation. In agreement with reduced CBP, the expression of CREB/CBP target genes related to memory, such *c-fos, Arc* and *Nr4a2*, was significantly reduced in the hippocampus of $Hdh^{Q7/Q111}$ mice compared with wild-type mice. Finally, and consistent with a role of CBP in cognitive impairment in $Hdh^{Q7/Q111}$ mice, administration of the histone deacetylase inhibitor trichostatin A rescues recognition memory deficits and transcription of selective CREB/CBP target genes in $Hdh^{Q7/Q111}$ mice. These findings demonstrate an important role for CBP in cognitive dysfunction in HD and suggest the use of histone deacetylase inhibitors as a novel therapeutic strategy for the treatment of memory deficits in this disease.

INTRODUCTION

Cognitive impairment is an early clinical feature of Huntington's disease (HD), a neurodegenerative disorder caused by an expanded CAG repeat in the *huntingtin* gene, that often appear before the onset of motor symptoms or neuronal loss (1–4). Deficits in synaptic plasticity and memory have also been described in different mouse models of HD (5–9), although the precise molecular mechanisms underlying these memory deficits remain largely unknown.

Activity-induced gene transcription is required for hippocampal synaptic plasticity and memory consolidation (10,11). Compelling evidence indicate that the transcription factor c-AMP-responsive element binding protein (CREB) is essential for activity-induced gene expression mediating memory formation (12). CREB transcriptional activity depends on CREB phosphorylation and recruitment of specific co-activators (13). CREB-binding protein (CBP) is a transcriptional co-activator that regulates CREB-mediated transcription by enhancing the ability of phosphorylated CREB to activate expression of specific genes (14–16). CBP also acts as a histone acetyltransferase (HAT) to alter chromatin structure allowing gene transcription (17–19). Thus, CBP plays a dual role in CREB-mediated gene transcription as a scaffolding protein to recruit CREB and as a HAT protein acetylating histones to disrupt repressive chromatin structure (20).

*To whom correspondence should be addressed at: Universitat de Barcelona, Casanova 143, E-08036 Barcelona, Spain. Tel: +34 934035284; Fax: +34 934021907; Email: silviagines@ub.edu
†The authors wish it to be known that, in their opinion, the first two authors should be regarded as joint First Authors.

Recent studies have revealed a particular role of CBP HAT activity in memory consolidation. Mouse models in which CBP activity is compromised exhibited reduced chromatin acetylation and hippocampal long-term potentiation (LTP) and long-term memory deficits (21–23).

Loss of CBP function has been associated with striatal degeneration in HD models (24–27). Indeed, mutant huntingtin directly interacts with the acetyltransferase domain of CBP, which results in reduced acetyltransferase activity (28). Decreased striatal CBP levels either by sequestration into huntingtin nuclear aggregates or by increased protein degradation has been reported in HD cellular and mouse models and HD human brain (26,28–30). Consistent with deficient striatal CBP function, either CBP overexpression or histone deacetyl transferase (HDAC) inhibition prevent cell loss and increase cell survival in HD models (31,32). Altogether, these data point to an important role of CBP loss of function in polyglutamine-dependent striatal toxicity in HD. Surprisingly, the role of CBP in regulating gene expression required for memory in HD has not been investigated. In this study, we address an important gap in our knowledge of cognitive deficits in HD. We demonstrate long-term spatial and recognition memory deficits in $Hdh^{Q7/Q111}$ mutant mice associated with reduced hippocampal CBP levels and selective disruption of memory-related CREB/CBP-dependent genes. Consistent with functional disruption of CBP, we found that HDAC inhibition efficiently rescued expression of specific CREB target genes and memory deficits in $Hdh^{Q7/Q111}$ mutant mice. Together, these findings implicate CBP dysfunction in HD cognitive deficits and provide support for new therapeutic approaches targeting CBP/CREB signaling pathway for treating cognitive impairment in HD.

RESULTS

Long-term object recognition memory is impaired in $Hdh^{Q7/Q111}$ knock-in mutant mice

Memory and cognitive deficits are evident in HD even before the diagnosis of motor symptoms (1,2,4,33,34). To evaluate memory function in HD, spatial and recognition memories were analyzed in heterozygous knock-in $Hdh^{Q7/Q111}$ mice, a genetically precise model of HD in which expanded *HD* CAG repeats are inserted into the exon 1 of the mouse's *HD* gene (35). To assess recognition memory, we first measured the performance of wild-type $Hdh^{Q7/Q7}$ and mutant $Hdh^{Q7/Q111}$ mice at 4 and 8 months of age in the novel object recognition task (NORT) (Fig. 1). This test evaluates recognition memory by measuring the innate tendency of mice to preferentially explore a novel object. Control $Hdh^{Q7/Q7}$ and $Hdh^{Q7/Q111}$ mutant mice were allowed to explore objects for 10 min during the training period showing no significant differences between genotypes at 4 or 8 months of age ($P > 0.05$) (Fig. 1A and B). At 15 min post-training, both $Hdh^{Q7/Q111}$ mutant and $Hdh^{Q7/Q7}$ wild-type mice spent significantly more time exploring the novel object at either 4 months ($P < 0.001$) or 8 months of age ($P < 0.05$ and $P < 0.001$), which indicates preserved short-term recognition memory in HD mice (Fig. 1A and B). In contrast, and compared with $Hdh^{Q7/Q7}$ wild-type mice, 8-month-old $Hdh^{Q7/Q111}$ mutant mice had a significant lower preference for the novel object when tested 24 h after training ($Hdh^{Q7/Q7}$: familiar object 37 ± 5.6% and novel object 62 ± 5.6%, $P < 0.001$; $Hdh^{Q7/Q111}$: familiar object 45 ± 4.2% and novel object 53 ± 4.4%, $P = 0.102$) (Fig. 1B). These results demonstrate that $Hdh^{Q7/Q111}$ mutant mice exhibit normal short-term memory but age-dependent impairment of long-term recognition memory.

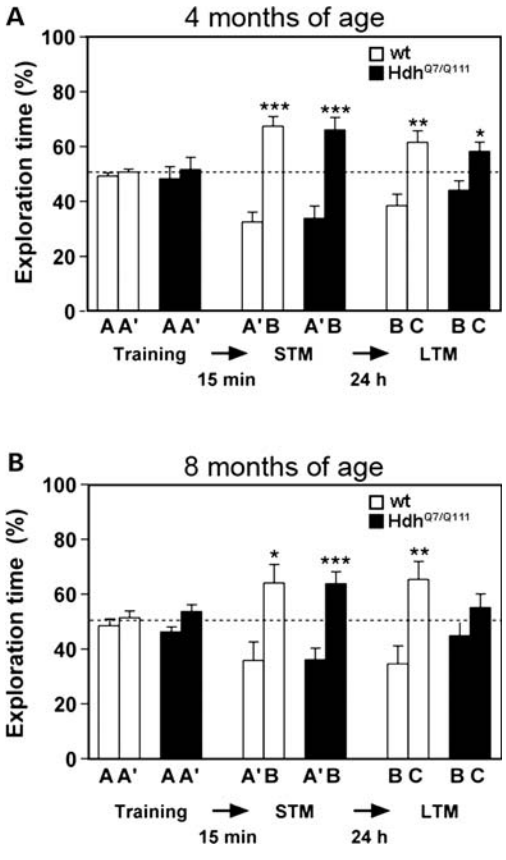

Figure 1. Impaired long-term recognition memory in mutant $Hdh^{Q7/Q111}$ knock-in mice. (**A**) Bar diagram illustrating the exploration time of $Hdh^{Q7/Q7}$ wild-type mice ($n = 6$) and $Hdh^{Q7/Q111}$ mutant mice ($n = 9$) at 4 months of age during the training, short-term (15 min delay, STM) and long-term (24 h delay, LTM) memory sessions in a NORT. Mice spent similar time exploring both objects during the training session. There was no significant difference in the percentage of exploration time between genotypes at either 15 min or at 24 h testing session. (**B**) Bar diagram illustrating the exploration time of $Hdh^{Q7/Q7}$ wild-type mice ($n = 6$) and $Hdh^{Q7/Q111}$ mutant mice ($n = 9$) at 8 months of age during the training, short-term (STM) and long-term (LTM) memory sessions in a NORT. Mice spent similar time exploring both objects during the training session. At 15 min post-training, both $Hdh^{Q7/Q111}$ mutant and $Hdh^{Q7/Q7}$ wild-type mice spent significantly more time exploring the novel object. However, during the 24 h retention test, $Hdh^{Q7/Q111}$ mutant mice displayed no significant preference for the novel object. Exploration time is shown in the bar graphs as mean ± SEM. $^{*}P < 0.05$, $^{**}P < 0.01$, $^{***}P < 0.001$ using a one-way ANOVA and Student *t*-test as a *post-hoc* test.

Hippocampal-dependent spatial memory deficits in $Hdh^{Q7/Q111}$ knock-in mutant mice

We next examined hippocampal-dependent spatial memory in $Hdh^{Q7/Q7}$ wild-type and $Hdh^{Q7/Q111}$ mutant mice at 8 months of age in the Morris water maze (MWM) task. Mice were first tested in the visible platform version of the MWM (four

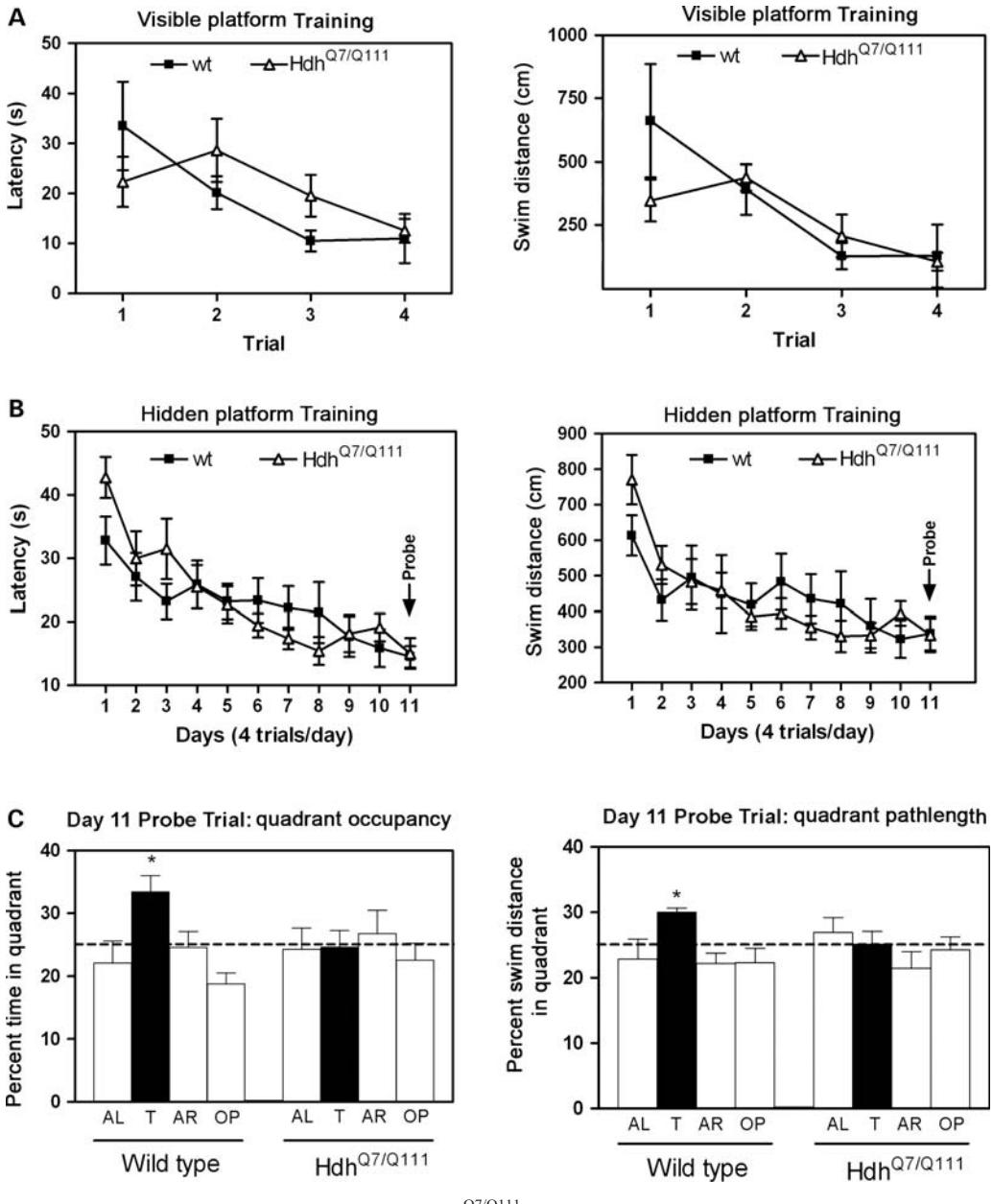

Figure 2. Impaired hippocampal-dependent spatial memory in mutant $Hdh^{Q7/Q111}$ knock-in mice. (**A**) In the visible platform task, mutant mice display similar escape latencies and path lengths than wild-type mice. A significant improvement across days was observed in both genotypes. (**B**) Eight-month-old $Hdh^{Q7/Q7}$ wild-type mice ($n = 6$) and $Hdh^{Q7/Q111}$ mutant mice ($n = 9$) were trained in the MWM task for 11 days. Both groups show similar average escape latencies and mean path-lengths with a significant improvement in their performances over training. (**C**) In the probe trial $Hdh^{Q7/Q111}$ mutant mice show no preference in occupancy (left) and swimming path-lengths (right) in the target quadrant compared with the rest of quadrants (T versus AL, AR, OP). AL, adjacent left; T, target quadrant; AR, adjacent right; OP, opposite quadrant. Data represent the mean ± SEM. Statistical analysis was performed using two-way ANOVA with repeated measures (A and B) and one-way ANOVA (C) followed by Newman–Keuls as a *post-hoc* test. $^{*}P < 0.05$, compared with the rest of quadrants.

trials per day) to control for visual ability and ensure that all mice were motivated and able to locate the platform. $Hdh^{Q7/Q111}$ mutant mice located the platform with similar escape latencies (trial effect: $F_{(3,52)} = 5.779$, $P < 0.01$; genotype effect: $F_{(1,52)} = 0.1739$, $P = 0.683$) and swimming path-lengths (trial effect: $F_{(3,52)} = 7.028$, $P < 0.001$; genotype effect: $F_{(1,52)} = 0.7512$, $P = 0.4$) than $Hdh^{Q7/Q7}$ wild-type mice, indicating that both groups improved significantly across trials (Fig. 2A).

When spatial learning was tested using the hidden platform version of the task, we found a significant improvement in their performances during training ($P < 0.001$) (Fig. 2B) with no significant differences between control $Hdh^{Q7/Q7}$ and mutant $Hdh^{Q7/Q111}$ mice in escape latencies (day effect: $F_{(10,150)} = 28.03$, $P < 0.001$; genotype effect: $F_{(1,\ 150)} = 0.11$, $P = 0.793$) or swimming path-lengths (day effect: $F_{(10,150)} = 25.34$, $P < 0.001$; genotype effect: $F_{(1,\ 150)} = 0.15$, $P = 0.606$). In the probe trial, in which the platform

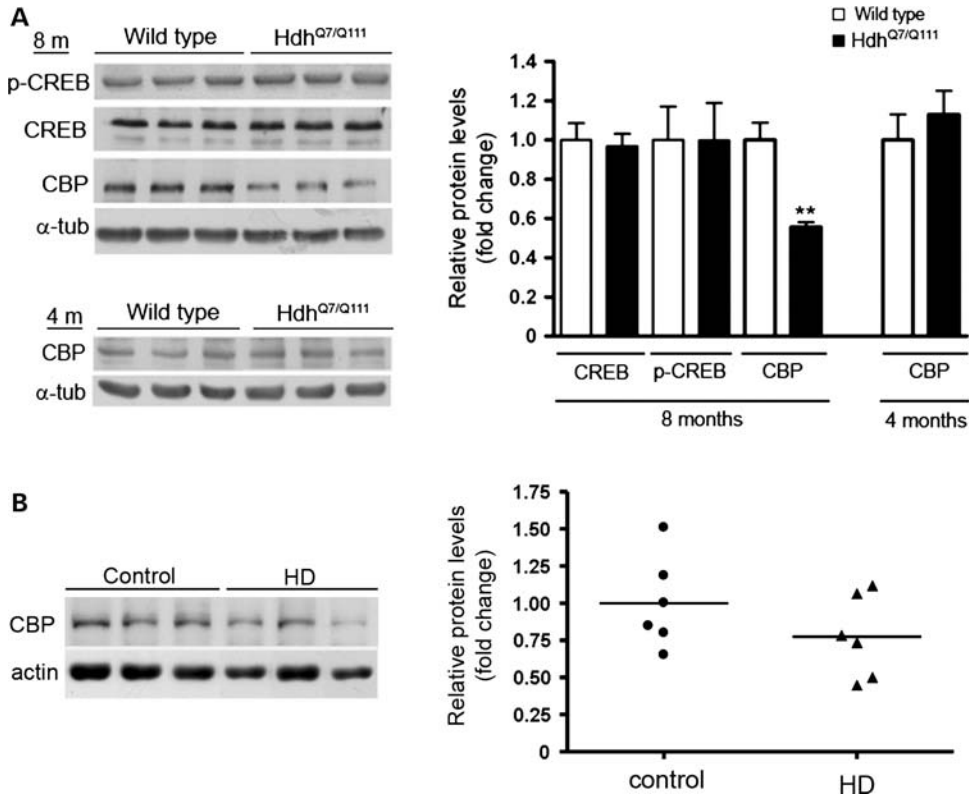

Figure 3. Reduced CBP protein levels in the hippocampus of mutant Hdh$^{Q7/Q111}$ mice and HD human brain. (**A**) Western blot (left) and quantification (right) showing similar levels of CREB and phosphorylated-CREB (Ser133) in total hippocampal extracts from mutant Hdh$^{Q7/Q111}$ mice compared with wild-type Hdh$^{Q7/Q7}$ mice at the age of 8 months. A significant reduction in CBP levels was also observed by western blot analysis in mutant mice at the age of 8 months when compared with wild-type mice, whereas no significant changes were detected at 4 months of age. Protein levels were normalized to α-tubulin as a loading control. The histogram represents the relative protein levels expressed as fold change of wild-type mice. Values are given as mean ± SEM of five independent samples. $^{**}P < 0.01$ mutant compared with wild-type mice using Student *t*-test. (**B**) Representative western blot showing levels of CBP and actin as a loading control from control and HD human hippocampal brain samples. Scatter plots represent the relative levels of CBP. The mean value of control samples was set as 1.

was removed, Hdh$^{Q7/Q111}$ mutant mice showed impaired spatial memory compared with Hdh$^{Q7/Q7}$ mice (Fig. 2C). Thus, whereas wild-type mice exhibited a preference for the target quadrant (quadrant effect: $F_{(3,\ 23)} = 5.406$, $P < 0.01$), evaluated as the time spent in the target quadrant versus each of the other quadrants, Hdh$^{Q7/Q111}$ mutant mice did not show such a preference (quadrant effect: $F_{(3,\ 35)} = 0.301$, $P = 0.824$). Moreover, Hdh$^{Q7/Q111}$ mutant mice displayed significantly less swimming path-lengths in the target quadrant compared with the rest of quadrants (quadrant effect: $F_{(3,\ 35)} = 1.080$, $P = 0.371$) than Hdh$^{Q7/Q7}$ mice (quadrant effect: $F_{(3,\ 23)} = 3.409$, $P < 0.05$) (Fig. 2C). Overall, these results demonstrate that Hdh$^{Q7/Q111}$ mutant mice exhibit normal acquisition of a MWM task but impaired hippocampal-dependent long-term spatial memory.

CBP is significantly reduced in the hippocampus of Hdh$^{Q7/Q111}$ knock-in mutant mice and in HD human brain

CBP/CREB signaling is critical for long-lasting changes in synaptic plasticity underlying long-term memory consolidation (11). To determine the molecular mechanisms underlying the observed long-term memory deficits in Hdh$^{Q7/Q111}$ mutant mice, we analyzed the levels of total CREB, phosphorylated CREB (Ser133) and CBP in hippocampal extracts from Hdh$^{Q7/Q7}$ wild-type and Hdh$^{Q7/Q111}$ mutant mice at the age of 8 months. Western blot analysis revealed similar levels of phosphorylated and total CREB, but a significant reduction in CBP protein levels in mutant compared with wild-type mice (~45%, $P < 0.01$; Fig. 3A). Importantly, at 4 months of age when no cognitive deficits were observed, unchanged CBP levels were found between Hdh$^{Q7/Q7}$ wild-type and Hdh$^{Q7/Q111}$ mutant mice (Fig. 3A). We also investigated the levels of CBP in hippocampal samples from HD patients. Western blot analysis revealed that CBP levels were notably lower, although no significant, than that in control brains (Fig. 3B), demonstrating that altered CBP levels are also manifested in HD patients.

We next examined whether reduced CBP levels were associated with diminished CBP mRNA expression. Quantitative real-time polymerase chain reaction (PCR) analysis showed no significant differences in mRNA *CBP* transcripts between wild-type and mutant huntingtin mice (Hdh$^{Q7/Q7}$: 1.0 ± 0.1 and Hdh$^{Q7/Q111}$: 1.1 ± 0.1), indicating that decreased CBP levels are not due to altered CBP transcription.

Depletion of CBP in the striatum of HD mice models has been associated with either recruitment of CBP into mutant huntingtin aggregates (26,28,30) or enhanced CBP degradation

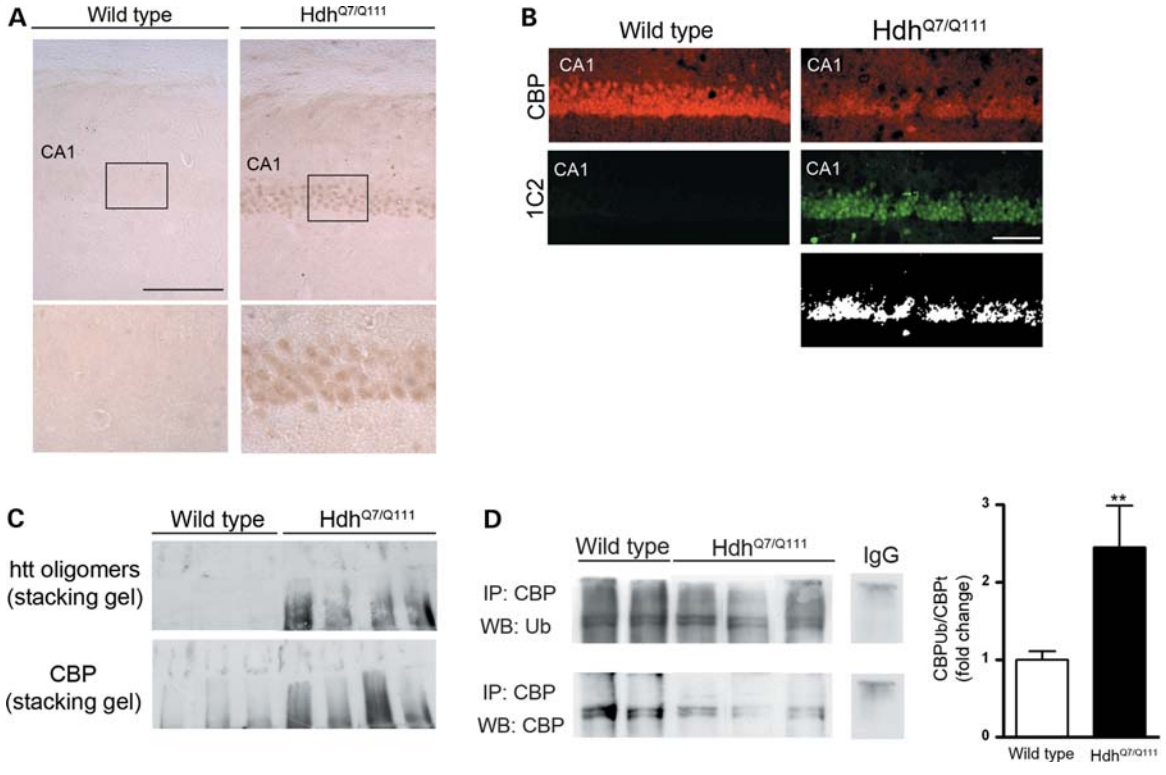

Figure 4. CBP reduction in the hippocampus of mutant Hdh$^{Q7/Q111}$ mice is associated with nuclear accumulation of mutant huntingtin and enhanced CBP ubiquitylation. (**A**) Intranuclear accumulation of mutant huntingtin in hippocampal neurons of the CA1 region in Hdh$^{Q7/Q111}$ mice. Immunostaining of coronal brain sections from wild-type Hdh$^{Q7/Q7}$ and mutant Hdh$^{Q7/Q111}$ mice at 8 months of age using the 1C2 antibody that selectively recognizes polyglutamine repeats in mutant huntingtin. Inset shows enlarged CA1 region. Scale bar 90 μm. (**B**). Immunostaining of coronal brain sections from wild-type Hdh$^{Q7/Q7}$ and mutant Hdh$^{Q7/Q111}$ mice at 8 months of age using CBP (red fluorescence) and 1C2 (green fluorescence) antibodies. Note the correlation between CBP and 1C2 distribution in mutant Hdh$^{Q7/Q111}$ mice (merged is shown in white). Scale bar 70 μm. (**C**) Western blotting of hippocampal extracts isolated from wild-type Hdh$^{Q7/Q7}$ and mutant Hdh$^{Q7/Q111}$ mice at the age of 8 months. The blots were probed with 1C2 for huntingtin and CBP antibodies. In samples from HD but not from wild-type mice, CBP was detected in the stacking gel. When the blot was stripped and reprobed with the 1C2 antibody, oligomeric forms of mutant huntingtin were also detected. (**D**) Enhancement of endogenous CBP ubiquitylation in the hippocampus of 8-month-old mutant Hdh$^{Q7/Q111}$ mice. Hippocampal extracts isolated from wild-type Hdh$^{Q7/Q7}$ and mutant Hdh$^{Q7/Q111}$ mice were subjected to immunoprecipitation with an anti-CBP antibody. Immunoprecipitates were analyzed by western blotting to detect ubiquitylated proteins and endogenous CBP. The ratio ubiquitilated CBP/total CBP was significantly increased in the hippocampus of mutant Hdh$^{Q7/Q111}$ mice. Data are presented as mean ± SEM of five independent samples. $^{**}P < 0.01$ using Student *t*-test.

(24,29,36). Therefore, we first tested the hypothesis that the observed reduction in soluble CBP was associated with the accumulation of nuclear mutant huntingtin in the hippocampus of Hdh$^{Q7/Q111}$ mutant mice. Immunohistochemical analysis in hippocampal tissue of mutant and wild-type mice at 8 months of age was performed using the 1C2 antibody that selectively recognize the expanded polyglutamine domain in mutant huntingtin (37,38). Extensive accumulation of nuclear mutant huntingtin detected as positive 1C2 immunoreactivity was found in the hippocampus of mutant Hdh$^{Q7/Q111}$ mice compared with Hdh$^{Q7/Q7}$ wild-type mice (Fig. 4A). We next determined by confocal microscopy whether 1C2 staining was associated with CBP immunoreactivity (Fig. 4B). In agreement with the biochemical analysis, an important reduction in CBP was found in the hippocampus of mutant compared with wild-type mice (Fig. 4B). Most importantly and consistent with our hypothesis, we found co-localization between CBP and 1C2 in the hippocampus of mutant Hdh$^{Q7/Q111}$ mice. Because soluble CBP was reduced in the hippocampus of Hdh$^{Q7/Q111}$ mutant mice and CBP was found to co-localize with nuclear mutant huntingtin, we next studied the presence of aggregated forms of huntingtin and CBP in the stacking gel of western blots (Fig. 4C). 1C2 immunostaining revealed oligomeric huntingtin forms detected as a diffuse smear in lysates from mutant but not wild-type mice. Notably, when immunoblots were reprobed with a CBP antibody, a similar large smear in the stacking gel was found in mutant mice samples. These results suggest that decreased CBP protein levels are associated with nuclear accumulation of mutant huntingtin in the hippocampus of Hdh$^{Q7/Q111}$ mutant mice.

However, enhanced CBP degradation could also provide another mechanism involved in the observed decrease in CBP levels in mutant mice. To explore this possibility, we analyzed the levels of ubiquitinated CBP immunoprecipitated from Hdh$^{Q7/Q7}$ wild-type and Hdh$^{Q7/Q111}$ mutant hippocampal extracts (Fig. 4D). Detection of immunocomplexes with an anti-ubiquitin antibody revealed a significant increase in ubiquitilated CBP/total CBP levels (~2.5-fold, $P < 0.01$) in mutant compared with wild-type mice, which is consistent with the idea that increased proteosomal-dependent ubiquitination and degradation of CBP could also be involved in the CBP reduction detected in the hippocampus of Hdh$^{Q7/Q111}$ mutant mice.

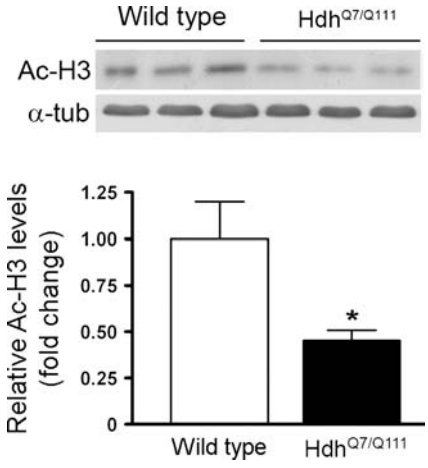

Figure 5. Decreased levels of CBP were associated with reduced acetylation of histone H3 in the hippocampus of mutant Hdh$^{Q7/Q111}$ mice. Western blot and quantification showing a significant reduction in Ac-H3 levels in total hippocampal extracts from mutant Hdh$^{Q7/Q111}$ mice compared with wild-type Hdh$^{Q7/Q7}$ mice at the age of 8 months. Protein levels were normalized to α-tubulin as a loading control. The histograms represent the relative protein levels expressed as fold change of wild-type mice. Values are given as mean ± SEM of five to seven independent samples. $^{*}P < 0.05$ using Student *t*-test.

Reduced acetylation of histone H3 in the hippocampus of Hdh$^{Q7/Q111}$ knock-in mutant mice

Since histone acetylation is significantly reduced in CBP heterozygous or conditional knock-out mice (21–23) and CBP HAT activity is essential for the conversion of short-term to long-term memory (39,40), we next tested whether reduced CBP could involve decreased histone acetylation in the hippocampus of HD mutant mice. We examined acetylation levels of histone H3 in the hippocampus of wild-type and mutant mice at 8 months of age by western blot analysis (Fig. 5). A significant decrease (∼55%, $P < 0.05$) in acetylated H3 histone levels was detected in the hippocampus of Hdh$^{Q7/Q111}$ mutant mice compared with Hdh$^{Q7/Q7}$ wild-type mice. These data suggest that altered histone acetylation due to reduced CBP activity could contribute to cognitive deficits in Hdh$^{Q7/Q111}$ mice.

Down-regulation of CREB/CBP-dependent genes in Hdh$^{Q7/Q111}$ knock-in mutant mice

Chromatin modification via CBP-mediated histone acetylation is an important molecular pathway involved in the regulation of CREB-dependent gene transcription underlying long-term memory formation (11). To determine whether altered CREB-dependent transcription contributes to cognitive deficits in Hdh$^{Q7/Q111}$ mutant mice, we analyzed by quantitative real-time PCR the expression of well-established CREB–CBP target genes in the hippocampus of spatial-trained wild-type Hdh$^{Q7/Q7}$ and mutant Hdh$^{Q7/Q111}$ mice at the age of 8 months. A significant reduction in CREB target genes related to synaptic plasticity and memory such as *c-fos* (∼36%), *Arc* (∼32%) or *Nr4a2* (∼25%) but not of CREB-dependent genes associated with cell proliferation (*Cyr61*) or stress (*Fosb*) was detected in the hippocampus of trained

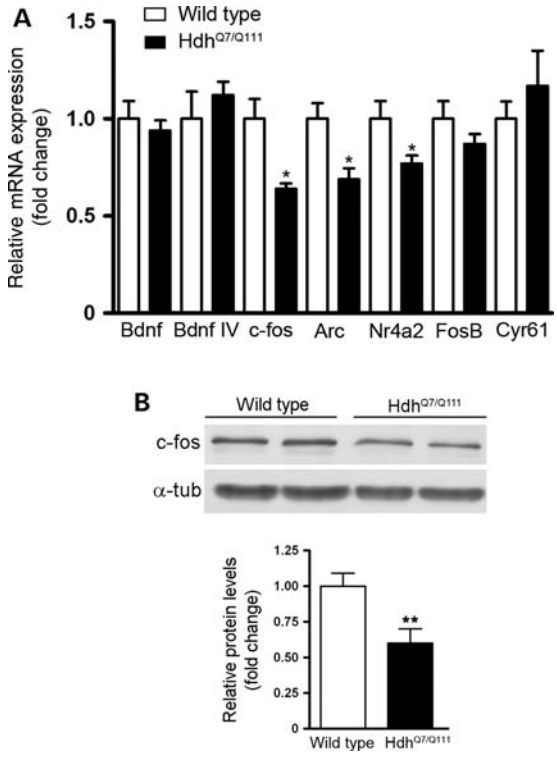

Figure 6. Reduced CREB/CBP-dependent gene transcription in Hdh$^{Q7/Q111}$ mutant mice following MWM training. (**A**) Quantitative real-time RT–PCR analysis performed in hippocampal samples of 8-month-old Hdh$^{Q7/Q7}$ wild-type ($n = 6$) and Hdh$^{Q7/Q111}$ mutant ($n = 7$) mice following MWM training. qRT–PCR analysis reveals significant reduction in the CREB target genes, *c-fos*, *Arc* and *Nr4a2* in Hdh$^{Q7/Q111}$ mutant mice compared with wild-type mice. mRNA expression is expressed as fold change values of wild-type mice normalized to GAPDH and 18S. $^{*}P < 0.05$ compared with wild-type mice. (**B**) Western blot images (top) and quantification (bottom) showing reduced c-fos protein levels in the hippocampus of trained Hdh$^{Q7/Q111}$ mutant mice ($n = 7$) compared with Hdh$^{Q7/Q7}$ wild-type mice ($n = 6$). Protein levels were normalized to α-tubulin as a loading control. The histogram represents the relative protein levels expressed as fold change of wild-type mice. Values are given as mean ± SEM. $^{**}P < 0.01$ compared with wild-type mice using Student *t*-test.

Hdh$^{Q7/Q111}$ mutant mice (Fig. 6A). Notably, reduced expression of *c-fos* mRNA was associated with a significant decrease in c-fos protein levels (∼40%, $P < 0.01$) (Fig. 6B). These results demonstrate selective reduction in CREB target genes in the hippocampus of memory impaired Hdh$^{Q7/Q111}$ mutant mice, suggesting that deficient CREB/CBP-dependent gene transcription may account for the impaired hippocampal-dependent memory observed in these mice.

HDAC inhibition rescues long-term memory deficits in Hdh$^{Q7/Q111}$ knock-in mutant mice

To further examine the possibility that CBP HAT activity was indeed involved in long-term memory deficits in mutant Hdh$^{Q7/Q111}$ mice, we next tested whether cognitive deficits could be ameliorated by a general increase in histone acetylation. To this aim we used trichostatin A (TSA), a well-known HDAC inhibitor that increases histone acetylation in cell culture and mouse models without evident toxicity (40–42). To determine whether TSA treatment improves long-term

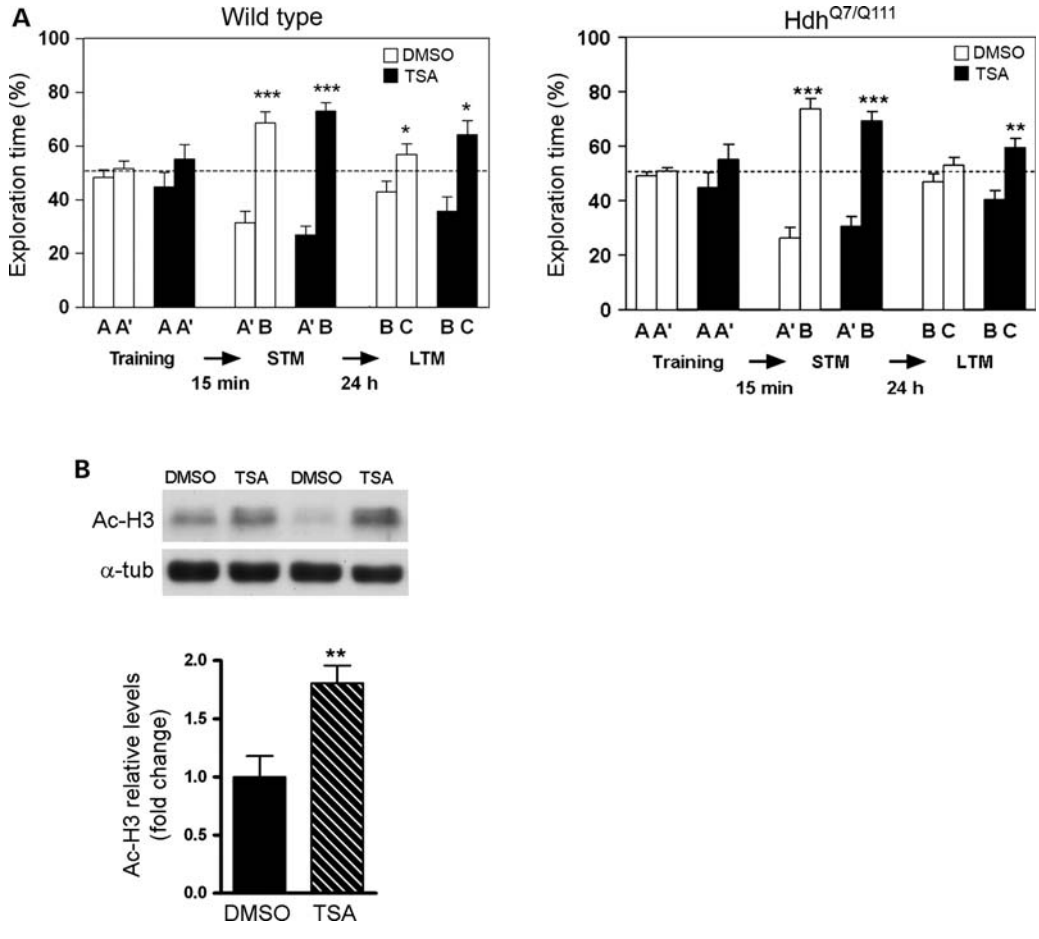

Figure 7. Administration of the histone deacetylase inhibitor TSA reverses recognition memory deficits in mutant Hdh$^{Q7/Q111}$ mice. TSA administration 2 h before training rescued recognition memory deficits in mutant Hdh$^{Q7/Q111}$ mice. (**A**) Bar diagram illustrating the exploration time for wild-type Hdh$^{Q7/Q7}$ ($n = 5$) (left) and mutant Hdh$^{Q7/Q111}$ ($n = 6$) (right) mice during the training, short-term (15 min delay, STM) and long-term (24 h delay, LTM) memory sessions in a NORT. TSA treatment does not affect mice performance during the training session and at 15 min post-training (short-term memory). However, TSA-treated mutant Hdh$^{Q7/Q111}$mice exhibited significantly enhanced preference for the novel object compared with the vehicle-treated Hdh$^{Q7/Q111}$ mice 24 h after training (long-term memory). Exploration time is shown in the bar graphs as mean ± SEM. $^{*}P < 0.05$, $^{**}P < 0.01$, $^{***}P < 0.001$ in a one-way ANOVA with Student *t*-test as a *post-hoc* test. (**B**) Western blot and quantification showing a significant increase in Ac-H3 levels in total hippocampal extracts from TSA-treated mutant Hdh$^{Q7/Q111}$ mice compared with DMSO-treated mutant Hdh$^{Q7/Q111}$ mice following NORT task. Protein levels were normalized to α-tubulin as a loading control. The histograms represent the relative protein levels expressed as fold change of DMSO-treated mutant mice. Values are given as mean ± SEM of six independent samples. $^{**}P < 0.01$ using Student *t*-test.

memory deficits in Hdh$^{Q7/Q111}$ mutant mice, we examined the effect of TSA injection on memory by using the NORT test (Fig. 7A). To assess short- and long-term memory, we tested mice at two different retention intervals of 15 min and 24 h. In agreement with the above results (Fig. 1), we found no significant differences in performance between groups at 15 min, indicating that TSA did not affect short-term memory acquisition in both experimental groups (Fig. 7A). Interestingly, when object recognition memory was tested 24 h after training, TSA-treated mutant Hdh$^{Q7/Q111}$ mice exhibited significantly increased preference for the novel object compared with vehicle-treated-Hdh$^{Q7/Q111}$ mice (Hdh$^{Q7/Q111}$ TSA, familiar object: 39 ± 3.5% versus novel object: 60.5 ± 3.5%, $P < 0.01$; Hdh$^{Q7/Q111}$ vehicle, familiar object: 47 ± 3.2% versus novel object: 53 ± 3%, $P = 0.17$) (Fig. 7A). No significant differences were found between vehicle and TSA-treated wild-type Hdh$^{Q7/Q7}$ mice. Consistent with an improvement of long-term recognition memory in Hdh$^{Q7/Q111}$ mutant mice, a significant increase (~80%, $P < 0.01$) in acetylated histone H3 levels (AcH3) were found in TSA-treated Hdh$^{Q7/Q111}$ mutant mice compared with those treated with dymethyl sulfoxide (DMSO) (Fig. 7B). Altogether, these results suggest that reduced CBP HAT activity likely contributes to long-term cognitive deficits in Hdh$^{Q7/Q111}$ mutant mice and that TSA efficiently reverses histone acetylation and long-term object recognition memory deficits in HD mutant mice.

Selective increase in CREB target genes in Hdh$^{Q7/Q111}$ knock-in mutant mice by HDAC inhibition

We next tested whether rescue of memory deficits in Hdh$^{Q7/Q111}$ mutant mice by TSA treatment was associated with enhanced expression of CREB/CBP-dependent genes. Quantitative real-time PCR analysis revealed that TSA-treated mutant mice exhibited a slight, but not statistically significant increase in *Arc* expression that was not observed in wild-type mice.

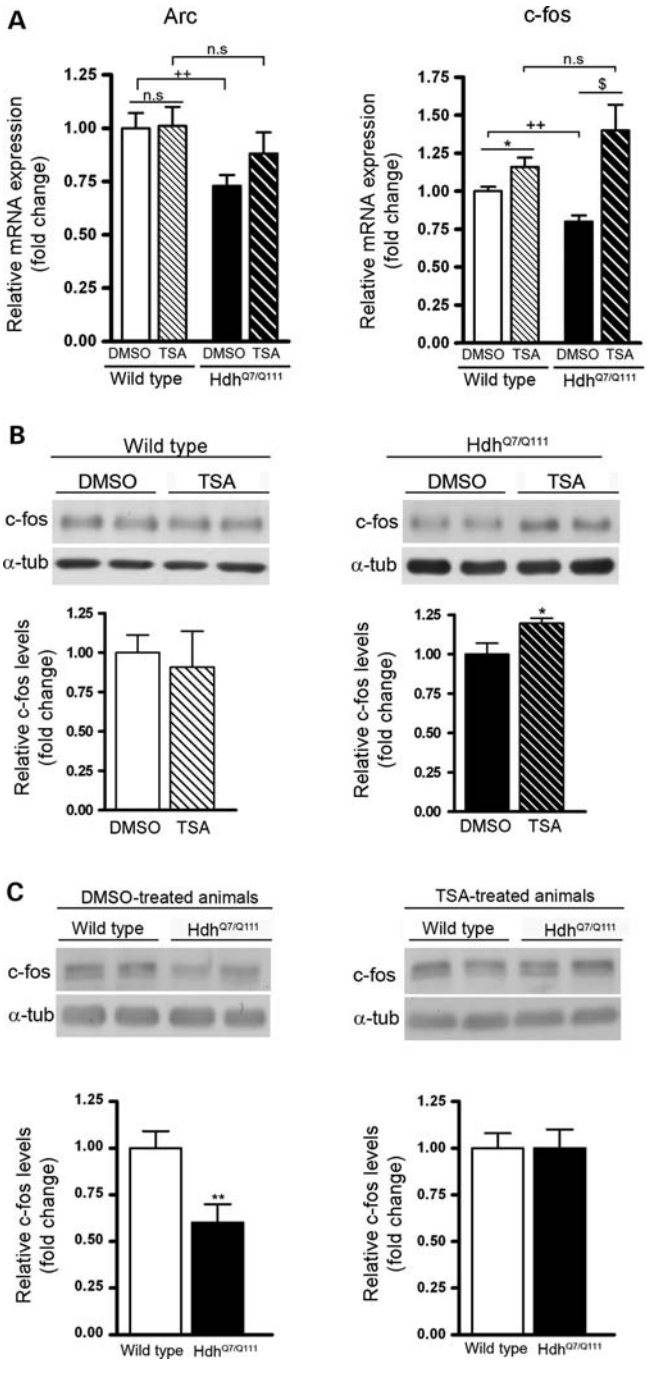

Figure 8. Increase in selective CREB target genes by TSA administration in $Hdh^{Q7/Q111}$ knock-in mutant mice. (**A**) Quantitative real-time RT–PCR analysis performed in hippocampus of TSA-treated and DMSO-treated wild-type $Hdh^{Q7/Q7}$ and mutant $Hdh^{Q7/Q111}$ mice following NORT task. mRNA expression is expressed as the fold change values of the wild-type vehicle-treated mice. $^{*}P < 0.05$, TSA-treated wild-type mice compared with DMSO-treated wild-type mice. $^{++}P < 0.01$ DMSO-treated wild-type mice compared with DMSO-treated mutant mice, $^{\$}P < 0.05$ TSA-treated mutant mice compared with DMSO-treated mutant mice. (**B**) Western blot and quantification showing hippocampal c-fos protein levels from DMSO or TSA-treated wild-type $Hdh^{Q7/Q7}$ (left) and mutant $Hdh^{Q7/Q111}$ mice (right) following NORT task. Protein levels were normalized to α-tubulin as a loading control. The histograms represent the relative protein levels expressed as fold change of DMSO-treated mice. Values are given as mean ± SEM of five independent samples. $^{*}P < 0.05$ compared with DMSO-treated mutant mice using Student *t*-test. (**C**) Western blot images showing hippocampal c-fos protein levels from vehicle (left) and TSA (right) -treated wild-type $Hdh^{Q7/Q7}$ and mutant $Hdh^{Q7/Q111}$ mice following NORT task. Protein levels were normalized to α-tubulin as a loading control. The histograms represent the relative protein levels expressed as fold change of wild-type mice. Values are given as mean ± SEM of five to eight independent samples. $^{**}P < 0.01$ mutant compared with wild-type mice using Student *t*-test.

However, it is important to notice that when TSA-treated mice were compared no significant differences in *Arc* expression were detected, while a significant reduction was still found in DMSO-treated mice (~30% $P < 0.01$, Fig. 8A). Notably, while TSA treatment induced a drastic increase in *c-fos* expression in $Hdh^{Q7/Q111}$ mutant mice (~50%, $P < 0.05$), the increase was much moderate in $Hdh^{Q7/Q7}$ wild-type mice (~20%, $P < 0.05$). In agreement with these data, western blot analysis revealed that c-fos protein levels were significantly increased (~20%, $P < 0.05$) in TSA-treated mutant mice compared with those treated with DMSO, although no differences were found in wild-type mice (Fig. 8B). Consistently, when DMSO-treated mice were compared, a significant decrease in c-fos protein levels was found in mutant compared to wild-type mice (~44%, $P < 0.05$, Fig. 8C), while no significant differences were found between TSA-treated mice. Unfortunately, we failed to detect any specific band for Arc in hippocampal samples.

Altogether, these findings suggest that TSA treatment rescues long-term recognition memory deficits in mutant $Hdh^{Q7/Q111}$ mice likely by enhancing the expression of specific CREB/CBP-target genes relevant for long-term synaptic plasticity and memory.

DISCUSSION

Memory and cognitive deficits are clinical features of HD that are present at early disease stages, when motor symptoms are not yet evident (1,3,43–47). Image analysis indicates anatomic and functional brain atrophy in regions involved in cognitive function in pre-symptomatic HD patients (34,48–51), although the pathological and molecular mechanisms underlying cognitive deficits in this motor disorder are largely unknown. In this study, we provide evidence for the first time that diminished CBP levels and altered CREB/CBP-dependent transcription are associated with long-term memory deficits in heterozygous $Hdh^{Q7/Q111}$ mutant mice, a genetic model of HD that accurately express the *HD* CAG mutation.

Our behavioral data demonstrate that $Hdh^{Q7/Q111}$ mutant mice exhibit age-dependent long-term object recognition and spatial memory deficits but preserved short-term memory, which is consistent with previous reports showing impaired hippocampal LTP and spatial learning in HD mouse models (5–7,9,52–54). Moreover, we found that $Hdh^{Q7/Q111}$ mutant mice display normal acquisition but impaired consolidation of recognition and spatial memories in contrast with previous studies showing learning impairments in exon-1 HD mice (6,7,53). A more severe phenotype of exon-1 over-expressing transgenic HD mice compared with $Hdh^{Q7/Q111}$ knock-in mice may explain this apparent discrepancy.

To elucidate the specific molecular mechanism(s) underlying these memory deficits, we focused on CREB signaling, a pathway critical for hippocampal-dependent synaptic plasticity and long-term memory (14,55). We found reduced levels of CBP but unchanged levels of total and phosphorylated CREB in the hippocampus of $Hdh^{Q7/Q111}$ mutant mice at 8 months of age when memory deficits are present. Importantly, CBP levels remain unaltered in $Hdh^{Q7/Q111}$ mutant mice at 4 months, an age in which cognitive impairments are not observed. Consistent with these findings, we also observed reduced CBP levels in the hippocampus of HD patients, which support the idea that CBP dysfunction plays a relevant role in HD memory deficits.

Several possible mechanisms may account for the CBP reduction in the hippocampus of $Hdh^{Q7/Q111}$ mice. Our data indicate that mutant huntingtin does not regulate CBP expression at the transcriptional level but at the protein level. Thus, our findings showing intranuclear accumulation of mutant huntingtin in the hippocampus of $Hdh^{Q7/Q111}$ mutant mice as well as an association of CBP with oligomeric forms of mutant huntingtin suggest that similarly to that observed in the striatum (26,28,30), mutant huntingtin may interferes with hippocampal CBP function by reducing the levels of soluble CBP. However, in addition to depletion of soluble CBP, increased CBP-mediated proteasomal degradation may also contribute to reducing CBP. Indeed, it has been reported in hippocampal cell lines that mutant huntingtin selectively enhances CBP processing by the ubiquitin–proteasome pathway (24,36). Consistent with these studies, we found increased CBP ubiquitylation in the hippocampus of 8-month-old $Hdh^{Q7/Q111}$ mutant mice. Thus, collectively our data suggest that mutant huntingtin may alter hippocampal CBP levels via at least two different mechanisms: (i) reduction of soluble CBP and (ii) increased CBP degradation.

Loss of CBP function in the hippocampus has been extensively associated with defects in long-lasting synaptic plasticity and long-term memory in different experimental mouse models of psychiatric and cognitive disorders (21,22,40,42,56). The activity of CBP as transcriptional co-activator is essential for regulation of genes underlying memory formation (57,58) and its complete or partial inactivation in mutant mice causes impaired long-term memory without changes in learning and short-term memory (21,40,59,60). Consistent with the above results, we found that reduced CBP levels in the hippocampus of $Hdh^{Q7/Q111}$ mutant mice were associated with selective deregulation of CREB/CBP-target genes related to synaptic plasticity and memory (*c-fos, Nr4a2* and *Arc*) but not to cell proliferation (*Cyr61*) or stress (*Fosb*). Interestingly, decreased CRE-dependent gene expression as a consequence of diminished CBP levels or function is associated with synaptic plasticity and memory deficits in Alzheimer's disease mouse models (56,61,62) and inactivation or reduction of *Arc* or *c-fos* in the hippocampus results in deficits in spatial memory (63,64).

Besides genetic activation, epigenetic modifications and chromatin remodeling are essential mechanisms for proper cognitive functions (65–68). Histone modifications are especially relevant for transcriptional regulation during memory consolidation (69,70). In this view, CBP HAT activity has emerged as a critical component for synaptic plasticity and long-term memory (21,40,60,71). Thus, in several mouse models of cognitive dysfunction, diminished H3 acetylation has been associated with reduced CBP expression and/or activity (22,40,72). Consistent with these studies, we found a significant decrease in histone H3 acetylation in the hippocampus of $Hdh^{Q7/Q111}$ mutant mice providing the first demonstration of reduced H3 acetylation associated with memory deficits in a HD mouse model. If decreased histone acetylation contributes to memory dysfunction in $Hdh^{Q7/Q111}$ mutant mice, we would expect that HDAC inhibitors improve these cognitive deficits. Consistent with this hypothesis, we found that HDAC inhibition by TSA treatment efficiently reversed long-term memory impairments in $Hdh^{Q7/Q111}$ mutant mice. This result agrees with recent reports showing that HDAC inhibitors enhance synaptic plasticity and improve memory deficits in different mouse models of cognitive dysfunction (21,22,73–77). Importantly, HDAC inhibition rather than having a general effect in gene expression positively affects the transcription of specific genes involved in memory consolidation (42,75,78). Interestingly, we found that TSA treatment increases the expression of *c-fos* and *Arc* in mutant $Hdh^{Q7/Q111}$ mice resulting in similar *c-fos* and *Arc* expression between genotypes. The critical involvement of c-fos and Arc in spatial and recognition memory consolidation has been largely demonstrated (63,64,79–81). Thus, impaired long-term memory and reduced LTP have been found in mice or rats lacking *c-fos* or *Arc* expression (63,64) and increased c-fos levels following systemic administration of HDAC inhibitors was associated with improvement of cognitive deficits in mouse models of neurodegenerative and cognitive disorders (82,83). Altogether, our results suggest that HDAC inhibition by TSA rescue memory deficits in $Hdh^{Q7/Q111}$ mutant mice by reducing histone acetylation deficits and enhancing transcription of specific CRE-target genes related to memory. However, we cannot rule out that non-histone substrates might also be affected by TSA treatment and therefore contribute to memory improvement in HD mice. Interestingly, it has been recently reported that TSA treatment compensates for the reduction in tubulin acetylation observed in HD neuronal models leading to improvement of axonal transport deficits and the subsequent release of brain-derived neurotrophic factor (BDNF) (84).

In summary, we show evidence that reduced hippocampal CBP levels may contribute to cognitive deficits in $Hdh^{Q7/Q111}$ mice by deregulating CREB-dependent transcription of specific genes involved in synaptic plasticity and memory. Likely, both reduced CBP transcriptional and HAT activities play a critical role in long-term memory impairments in $Hdh^{Q7/Q111}$ mice. Finally, the recovery of memory deficits in $Hdh^{Q7/Q111}$ mice by a HDAC inhibitor may have important therapeutic implications for treatment of cognitive deficits in HD.

MATERIALS AND METHODS

Reagents and antibodies

HDAC inhibitor TSA was obtained from Sigma-Aldrich. CBP (A22 and C-1) and c-fos (A4) antibodies were purchased from Santa Cruz Biotechnology. Phospho-CREB (Ser133), CREB

and acetyl-H3 (C5B11) antibodies were from Cell Signaling Technologies. 1C2 antibody and 2166 antibody were obtained from Millipore. Ubiquitin antibody was from Abcam. Anti-tubulin and anti-actin were from Sigma-Aldrich.

Huntington's disease mouse model

Hdh^{Q111} knock-in mice, with targeted insertion of 109 CAG repeats that extends the glutamine segment in murine huntingtin to 111 residues, were maintained on a C57BL/6 genetic background (35). $Hdh^{Q7/Q111}$ heterozygous males and females were intercrossed to generate age-matched $Hdh^{Q7/Q111}$ heterozygous and $Hdh^{Q7/Q7}$ wild-type littermates. Only males were used for all experiments. All procedures were carried out in accordance with the National Institute of Health and were approved by the local animal care committee of the Universitat de Barcelona (99/01) and the Generalitat de Catalunya (00/1094).

Postmortem brain tissue

Hippocampal brain tissues (six controls and six HD patients) were obtained from Banc de Teixits Neurològics (Servei Científico-Tècnic, Universitat de Barcelona, Barcelona, Spain) following the guidelines of the local ethics committees. Controls (mean ± SEM; age 53.5 ± 6.8 years; post-mortem intervals of 4–18 h), HD brain grades 3 and 4 (mean ± SEM; age 54.5 ± 6.5 years; post-mortem intervals of 4–17 h). Hippocampal brain tissue was homogenized in cold lysis buffer [20 mM Tris base (pH 8.0), 150 mM NaCl, 50 mM NaF, 1% NP-40, 10% glycerol and supplemented with 1 mM sodium orthovanadate and protease inhibitor cocktail (Sigma-Aldrich)], cleared by centrifugation at 16 000 *g* for 20 min and the supernatants collected and resolved on sodium dodecyl sulfate polyacrylamide gel electrophoresis (SDS–PAGE). CBP protein levels were finally determined by western blot analysis as described below. All the ethical guidelines contained within the latest Declaration of Helsinki were taken into consideration and informed consent was obtained from all subjects under study.

Behavioral learning tests

Novel object recognition test (NORT). The NORT has been adapted from a previously described protocol for rats (85). For the NORT task, mice were tested in a circular open field (40 cm diameter) located in a room with dim lighting. In the object recognition protocol, two different objects were placed in the circular field during the training phase. The objects varied in color, shape and size. To avoid olfactory cues, chamber and objects were thoroughly cleansed between trials. Briefly, 4- and 8-month-old male mice were habituated to the open field in the absence of the objects for 15 min each day over 3 days. During the training period, mice were placed in the open field with two identical objects for 10 min. Retention tests were performed either 15 min (short-term memory test) or 24 h (long-term memory test) after training by placing the mice back to the open field for a 5 min session and by randomly exchanging one of the familiar objects with a novel one. Training and testing trials were recorded and the time that mice spent exploring the novel and familiar objects was measured. Contact with a given object was defined as the mouse approaching the object nose first with the nose being within 1 cm of the object boarder. The relative exploration time was recorded and calculated using the formula ET = 100 × (new object inspection time/total inspection time). Experimenters were blind to the genotypes and treatment condition of the mice.

Morris water maze. Spatial learning was assessed in a MWM task modified for use in mice (7). Briefly, 8-month-old male mice were trained in a circular pool (diameter 100 cm; height 40 cm, water depth of 25 cm) four trials per day over 11 days. Four positions around the edge of the tank were arbitrarily designated as north (N), south (S), east (E), and west (W) to provide four alternative starting positions and to divide the tank into four quadrants: NE, SE, SW and NW. A circular white escape platform (10 cm in diameter) was submerged 1 cm below the water surface and placed at the midpoint of one of the four quadrants. The mouse was allowed to swim until it reached the platform or otherwise guided onto the platform after 60 s. Mice were left on the platform for 15 s before returned to the home cage during the inter-trial interval. On day 11, the mice performed a single 1 min probe trial without the platform 4 h after the last trial. The swim path of each mouse was recorded over 60 s, while it searched for the missing platform. Thirty minutes after the probe trial, mice were sacrificed by cervical dislocation and the hippocampus was rapidly dissected and frozen at −80°C. In the visible platform test, extramaze distal cues were removed, and the platform was marked with a high-contrast striped flag. The movement of the mice was monitored using an automated tracking system and data analyzed by the SMART junior software (Panlab, Spain). All experiments were performed by operators who were blind to the mice genotypes.

Real-time quantitative reverse transcriptase–PCR

Total RNA was isolated from hippocampus of heterozygous mutant and wild-type mice using the Total RNA Isolation Nucleospin® RNA II Kit (Macherey-Nagel, Düren, Germany). Purified RNA (500 ng) was reverse transcribed using the StrataScript® First Strand cDNA Synthesis System (Stratagene, Santa Clara, CA, USA). The cDNA synthesis was performed at 42°C for 60 min in a final volume of 20 μl according to the manufacturer's instructions. The cDNA was then analyzed by quantitative reverse transcriptase (RT)–PCR using the following TaqMan® Gene Expression Assays (Applied Biosystems, Foster City, CA, USA): 18S (Hs99999901_s1), Arc (Mn00479619_g1), c-Fos (Mn00487425_m1), BDNF (Mn00432069), Fosb (Mn_008036), Nr4a2 (Mn_013613.1) and Cyr61 (Mn_010516). RT–PCR was performed in 25 μl of final volume on 96-well plates, in a reaction buffer containing 12.5 μl TaqMan Gene Expression Assays and 20 ng of cDNA. Reactions included 40 cycles of a two-step PCR: 95°C for 30 s and 60°C for 1 min, after initial denaturation at 95°C for 10 min. All Q-PCR assays were performed in duplicate and repeated in at least three independent experiments. To provide negative controls and exclude contamination by genomic DNA, the RT was omitted in the cDNA synthesis step, and

the samples were subjected to the PCR reaction in the same manner with each TaqMan Gene Expression Assay. The Q-PCR data were analyzed using the MxPro™ Q-PCR analysis software version 3.0 (Stratagene). Quantification was performed with the Comparative Quantitation Analysis program of the mentioned software and using the 18S or glyceraldehyde 3-phosphatase dehydrogenase gene expression as internal controls.

Immunoprecipitation and western blot analysis

Heterozygous mutant $Hdh^{Q7/Q111}$ and wild-type $Hdh^{Q7/Q7}$ mice were killed by cervical dislocation at the age of 4 or 8 months. The brain was quickly removed, dissected, frozen in dry ice and stored at −80°C until use. Brain tissue was homogenized in cold lysis buffer [20 mM Tris base (pH 8.0), 150 mM NaCl, 50 mM NaF, 1% NP-40, 10% glycerol and supplemented with 1 mM sodium orthovanadate and protease inhibitor cocktail (Sigma-Aldrich)], cleared by centrifugation at 16 000 *g* for 20 min and the supernatants collected. Following determination of the protein contents by Detergent-Compatible Protein Assay (Bio-Rad, Hercules, CA, USA), protein extracts (20–60 μg) were mixed with 5× SDS sample buffer, boiled for 5 min, resolved on 6–10% SDS–PAGE and transferred to nitrocellulose membranes (Whatman Schleicher & Schuell, Keene, NH, USA). After incubation (30 min) in blocking buffer containing 10% non-fat powdered milk in Tris buffered saline-Tween (TBS-T) (50 mM Tris–HCl, 150 mM NaCl, pH 7.4, 0.05% Tween 20), membranes were blotted overnight at 4°C with primary antibodies: CBP (1:1000), CREB (1:1000), phospho-CREB (1:1000), acetyl-H3 (1:1000), c-fos (1:1000), 1C2 (1:1000), ubiquitin (1/50), anti-htt 2166 (1:1000), anti-actin (1:1000) or α-tubulin (1:50000). The membranes were then rinsed three times with TBS-T and incubated with horseradish peroxidase-conjugated secondary antibody for 1 h at room temperature. After washing for 30 min with TBS-T, the membranes were developed using the enhanced chemiluminescence ECL kit (Santa Cruz Biotechnology). The Gel-Pro densitometry program (Gel-Pro Analyzer for Windows, version 4.0.00.001) was used to quantify the different immunoreactive bands relative to the intensity of the α-tubulin band in the same membranes within a linear range of detection for the ECL reagent (86). Data are expressed as the mean ± SEM of band density.

Immunoprecipitation was performed by incubation of protein extracts (400 μg) obtained from hippocampus of 8-month-old wild-type $Hdh^{Q7/Q7}$ and mutant $Hdh^{Q7/Q111}$ mice with 3 μg of anti-CBP antibody (A-22) overnight at 4°C followed by a 2 h incubation with 30 μl of protein A-Sepharose Cl-4B (Sigma). The beads were washed by centrifugation three times, then resuspended in ice-cold phosphate buffered saline (PBS) and then boiled for 5 min for reducing SDS loading buffer. The immunocomplexes were resolved by SDS–PAGE on 8% polyacrylamide gel and transferred to nitrocellulose membranes. Immunoblot analysis was carried out as described above. Briefly, the blots were incubated with anti-CBP (C-1) and anti-ubiquitin and detected using ECL chemiluminescent reagents.

Trichostatin A administration

TSA was dissolved in 100% DMSO at a concentration of 2 μg/μl. For behavioral experiments, TSA or DMSO was administered by i.p. injection (1 μl/g body weight) 2 h before training on the NORT task. Training on the NORT task was followed by memory tests at 15 min and 24 h delays. To analyze c-fos levels, hippocampus from trained wild-type and mutant mice treated with vehicle or TSA were isolated and homogenized in cold lysis buffer as previously described, cleared by centrifugation at 16 000 *g* and the supernatants collected. Hippocampal extracts were resolved on 10% SDS–PAGE, transferred onto nitrocellulose membranes and immunoblot analysis carried out by incubation with c-fos antibody and detection using ECL chemiluminescent reagents.

Immunohistochemistry

For immunohistochemical analysis, heterozygous mutant $Hdh^{Q7/Q111}$ and wild-type $Hdh^{Q7/Q7}$ mice at 8 months of age ($n = 3$ for each condition) were deeply anesthetized and immediately perfused transcardially with saline followed by 4% paraformaldehyde/phosphate buffer. Brains were removed and postfixed for 1–2 h in the same solution, cryoprotected by immersion in 30% sucrose and then frozen in dry ice-cooled methylbutane. Serial coronal cryostat sections (30 μm) through the whole brain were collected in PBS as free-floating sections. Sections were rinsed three times in PBS and permeabilized and blocked in PBS containing 0.3% Triton X-100 and 3% normal goat serum (Pierce Biotechnology) for 15 min at room temperature. The sections were then washed in PBS and incubated overnight at 4°C with anti-1C2 (1:500) and anti-CBP (1:100) antibodies and detected with Cy3 anti-rabbit and Cy2 anti-mouse (1:200) secondary antibodies (Jackson ImmunoResearch). Following secondary antibody incubation, slices were rinsed in PBS and incubated with Hoechst solution (Invitrogen, 1:5000) for 10 min. As negative controls, some sections were processed as described in the absence of primary antibody and no signal was detected. Immunofluorescence was analyzed by confocal microscopy using a TCS SL laser scanning confocal spectral microscope (Leica Microsystems Heidelberg, Mannheim, Germany).

For detection of huntingtin, sections were pre-incubated with PBS containing 3% H_2O_2 for 45 min and blocked in 5% normal goat serum for 1 h. Sections were then incubated overnight at 4°C with 1C2 monoclonal antibody (1:500), washed three times in PBS and incubated with biotinylated secondary antibody (1:200; Pierce) at room temperature for 2 h and with avidin–biotin–peroxidase complex (ABC kit; Pierce). Reactions were visualized with diaminobenzidine as a chromagen. No signal was detected in controls in which the primary antibodies have been omitted. Light micrographs were obtained with an Olympus microscope BX51 (Olympus Danmark A/S).

Statistical analysis

Statistical analysis was performed using either Student's *t*-test or one-way analysis of variance (ANOVA) followed by Student's *t*-test. The MWM behavioral data were analyzed

using two-way ANOVA with repeated measures or one-way ANOVA followed by the Newman–Keuls test for *post hoc* comparisons. Data were shown as the mean ± SEM. Differences with $P < 0.05$ were considered significant.

ACKNOWLEDGEMENTS

We are very grateful to Ana Lopez and Maria Teresa Muñoz for technical assistance and Dr Teresa Rodrigo and the staff of the animal care facility (Facultat de Psicologia Universitat de Barcelona) for their help. We are grateful to the University of Barcelona and the Institute of Neuropathology Brain Banks (Barcelona, Spain) for providing hippocampal samples from control subjects and HD patients. We thank members of our laboratory for helpful discussion.

Conflict of Interest statement. None declared.

FUNDING

This work was supported by grants from Ministerio de Ciencia e Innovación (SAF2009-07077 to S.G., SAF2011-29507 to J.A. and SAF2010-20925 to C.A.S.); Centro de Investigaciones Biomédicas en Red sobre Enfermedades Neurodegenerativas (CIBERNED CB06/05/0054 and CB06/05/0042); Fondo de Investigaciones Sanitarias Instituto de Salud Carlos III (RETICS: RD06/0010/0006) and Fundació La Marató de TV3.

REFERENCES

1. Lawrence, A.D., Hodges, J.R., Rosser, A.E., Kershaw, A., ffrench-Constant, C., Rubinsztein, D.C., Robbins, T.W. and Sahakian, B.J. (1998) Evidence for specific cognitive deficits in preclinical Huntington's disease. *Brain*, **121**, 1329–1341.
2. Montoya, A., Pelletier, M., Menear, M., Duplessis, E., Richer, F. and Lepage, M. (2006) Episodic memory impairment in Huntington's disease: a meta-analysis. *Neuropsychologia*, **44**, 1984–1994.
3. Stout, J.C., Paulsen, J.S., Queller, S., Solomon, A.C., Whitlock, K.B., Campbell, J.C., Carlozzi, N., Duff, K., Beglinger, L.J., Langbehn, D.R *et al.* (2010) Neurocognitive signs in prodromal Huntington disease. *Neuropsychology*, **25**, 1–14.
4. Vonsattel, J.P. and DiFiglia, M. (1998) Huntington disease. *J. Neuropathol. Exp. Neurol.*, **57**, 369–384.
5. Brooks, S., Higgs, G., Jones, L. and Dunnett, S.B. (2010) Longitudinal analysis of the behavioural phenotype in Hdh(Q92) Huntington's disease knock-in mice. *Brain Res. Bull*., doi:10.106/j.brainresbull.2010.05.003.
6. Giralt, A., Rodrigo, T., Martin, E.D., Gonzalez, J.R., Mila, M., Cena, V., Dierssen, M., Canals, J.M. and Alberch, J. (2009) Brain-derived neurotrophic factor modulates the severity of cognitive alterations induced by mutant huntingtin: involvement of phospholipaseCgamma activity and glutamate receptor expression. *Neuroscience*, **158**, 1234–1250.
7. Lione, L.A., Carter, R.J., Hunt, M.J., Bates, G.P., Morton, A.J. and Dunnett, S.B. (1999) Selective discrimination learning impairments in mice expressing the human Huntington's disease mutation. *J. Neurosci.*, **19**, 10428–10437.
8. Lynch, G., Kramar, E.A., Rex, C.S., Jia, Y., Chappas, D., Gall, C.M. and Simmons, D.A. (2007) Brain-derived neurotrophic factor restores synaptic plasticity in a knock-in mouse model of Huntington's disease. *J. Neurosci.*, **27**, 4424–4434.
9. Simmons, D.A., Rex, C.S., Palmer, L., Pandyarajan, V., Fedulov, V., Gall, C.M. and Lynch, G. (2009) Up-regulating BDNF with an ampakine rescues synaptic plasticity and memory in Huntington's disease knockin mice. *Proc. Natl Acad. Sci. USA*, **106**, 4906–4911.
10. Barco, A., Pittenger, C. and Kandel, E.R. (2003) CREB, memory enhancement and the treatment of memory disorders: promises, pitfalls and prospects. *Expert Opin. Ther. Targets*, **7**, 101–114.
11. Kandel, E.R. (2001) The molecular biology of memory storage: a dialogue between genes and synapses. *Science*, **294**, 1030–1038.
12. Silva, A.J., Kogan, J.H., Frankland, P.W. and Kida, S. (1998) CREB and memory. *Annu. Rev. Neurosci.*, **21**, 127–148.
13. Rosenfeld, M.G. and Glass, C.K. (2001) Coregulator codes of transcriptional regulation by nuclear receptors. *J. Biol. Chem.*, **276**, 36865–36868.
14. Bourtchuladze, R., Frenguelli, B., Blendy, J., Cioffi, D., Schutz, G. and Silva, A.J. (1994) Deficient long-term memory in mice with a targeted mutation of the cAMP-responsive element-binding protein. *Cell*, **79**, 59–68.
15. Chrivia, J.C., Kwok, R.P., Lamb, N., Hagiwara, M., Montminy, M.R. and Goodman, R.H. (1993) Phosphorylated CREB binds specifically to the nuclear protein CBP. *Nature*, **365**, 855–859.
16. Ravnskjaer, K., Kester, H., Liu, Y., Zhang, X., Lee, D., Yates, J.R III and Montminy, M. (2007) Cooperative interactions between CBP and TORC2 confer selectivity to CREB target gene expression. *EMBO J.*, **26**, 2880–2889.
17. Kalkhoven, E. (2004) CBP and p300: HATs for different occasions. *Biochem. Pharmacol.*, **68**, 1145–1155.
18. Ogryzko, V.V., Schiltz, R.L., Russanova, V., Howard, B.H. and Nakatani, Y. (1996) The transcriptional coactivators p300 and CBP are histone acetyltransferases. *Cell*, **87**, 953–959.
19. Vo, N. and Goodman, R.H. (2001) CREB-binding protein and p300 in transcriptional regulation. *J. Biol. Chem.*, **276**, 13505–13508.
20. Chan, H.M. and La Thangue, N.B. (2001) p300/CBP proteins: HATs for transcriptional bridges and scaffolds. *J. Cell Sci.*, **114**, 2363–2373.
21. Alarcon, J.M., Malleret, G., Touzani, K., Vronskaya, S., Ishii, S., Kandel, E.R. and Barco, A. (2004) Chromatin acetylation, memory, and LTP are impaired in CBP+/− mice: a model for the cognitive deficit in Rubinstein-Taybi syndrome and its amelioration. *Neuron*, **42**, 947–959.
22. Chen, G., Zou, X., Watanabe, H., van Deursen, J.M. and Shen, J. (2010) CREB binding protein is required for both short-term and long-term memory formation. *J. Neurosci.*, **30**, 13066–13077.
23. Valor, L.M., Pulopulos, M.M., Jimenez-Minchan, M., Olivares, R., Lutz, B. and Barco, A. (2011) Ablation of CBP in forebrain principal neurons causes modest memory and transcriptional defects and a dramatic reduction of histone acetylation but does not affect cell viability. *J. Neurosci.*, **31**, 1652–1663.
24. Jiang, H., Poirier, M.A., Liang, Y., Pei, Z., Weiskittel, C.E., Smith, W.W., DeFranco, D.B. and Ross, C.A. (2006) Depletion of CBP is directly linked with cellular toxicity caused by mutant huntingtin. *Neurobiol. Dis.*, **23**, 543–551.
25. McCampbell, A., Taye, A.A., Whitty, L., Penney, E., Steffan, J.S. and Fischbeck, K.H. (2001) Histone deacetylase inhibitors reduce polyglutamine toxicity. *Proc. Natl Acad. Sci. USA*, **98**, 15179–15184.
26. Nucifora, F.C Jr, Sasaki, M., Peters, M.F., Huang, H., Cooper, J.K., Yamada, M., Takahashi, H., Tsuji, S., Troncoso, J., Dawson, V.L., Dawson, T.M. and Ross, C.A. (2001) Interference by huntingtin and atrophin-1 with cbp-mediated transcription leading to cellular toxicity. *Science*, **291**, 2423–2428.
27. Taylor, J.P., Taye, A.A., Campbell, C., Kazemi-Esfarjani, P., Fischbeck, K.H. and Min, K.T. (2003) Aberrant histone acetylation, altered transcription, and retinal degeneration in a Drosophila model of polyglutamine disease are rescued by CREB-binding protein. *Genes Dev.*, **17**, 1463–1468.
28. Steffan, J.S., Bodai, L., Pallos, J., Poelman, M., McCampbell, A., Apostol, B.L., Kazantsev, A., Schmidt, E., Zhu, Y.Z., Greenwald, M *et al.* (2001) Histone deacetylase inhibitors arrest polyglutamine-dependent neurodegeneration in Drosophila. *Nature*, **413**, 739–743.
29. Cong, S.Y., Pepers, B.A., Evert, B.O., Rubinsztein, D.C., Roos, R.A., van Ommen, G.J. and Dorsman, J.C. (2005) Mutant huntingtin represses CBP, but not p300, by binding and protein degradation. *Mol. Cell Neurosci.*, **30**, 12–23.
30. McCampbell, A., Taylor, J.P., Taye, A.A., Robitschek, J., Li, M., Walcott, J., Merry, D., Chai, Y., Paulson, H., Sobue, G. and Fischbeck, K.H. (2000) CREB-binding protein sequestration by expanded polyglutamine. *Hum. Mol. Genet.*, **9**, 2197–2202.
31. Ferrante, R.J., Kubilus, J.K., Lee, J., Ryu, H., Beesen, A., Zucker, B., Smith, K., Kowall, N.W., Ratan, R.R., Luthi-Carter, R. and Hersch, S.M.

(2003) Histone deacetylase inhibition by sodium butyrate chemotherapy ameliorates the neurodegenerative phenotype in Huntington's disease mice. *J. Neurosci.*, **23**, 9418–9427.
32. Gardian, G., Browne, S.E., Choi, D.K., Klivenyi, P., Gregorio, J., Kubilus, J.K., Ryu, H., Langley, B., Ratan, R.R., Ferrante, R.J. and Beal, M.F. (2005) Neuroprotective effects of phenylbutyrate in the N171–82Q transgenic mouse model of Huntington's disease. *J. Biol. Chem.*, **280**, 556–563.
33. Lawrence, A.D., Sahakian, B.J., Hodges, J.R., Rosser, A.E., Lange, K.W. and Robbins, T.W. (1996) Executive and mnemonic functions in early Huntington's disease. *Brain*, **119**, 1633–1645.
34. Montoya, A., Price, B.H., Menear, M. and Lepage, M. (2006) Brain imaging and cognitive dysfunctions in Huntington's disease. *J. Psychiatry Neurosci.*, **31**, 21–29.
35. Lloret, A., Dragileva, E., Teed, A., Espinola, J., Fossale, E., Gillis, T., Lopez, E., Myers, R.H., Macdonald, M.E. and Wheeler, V.C. (2006) Genetic background modifies nuclear mutant huntingtin accumulation and HD CAG repeat instability in Huntington's disease knock-in mice. *Hum. Mol. Genet.*, **15**, 2015–2024.
36. Jiang, H., Nucifora, F.C Jr, Ross, C.A. and DeFranco, D.B. (2003) Cell death triggered by polyglutamine-expanded huntingtin in a neuronal cell line is associated with degradation of CREB-binding protein. *Hum. Mol. Genet.*, **12**, 1–12.
37. Herndon, E.S., Hladik, C.L., Shang, P., Burns, D.K., Raisanen, J. and White, C.L III (2009) Neuroanatomic profile of polyglutamine immunoreactivity in Huntington disease brains. *J. Neuropathol. Exp. Neurol.*, **68**, 250–261.
38. Wang, J., Wang, C.E., Orr, A., Tydlacka, S., Li, S.H. and Li, X.J. (2008) Impaired ubiquitin-proteasome system activity in the synapses of Huntington's disease mice. *J. Cell Biol.*, **180**, 1177–1189.
39. Barrett, R.M. and Wood, M.A. (2008) Beyond transcription factors: the role of chromatin modifying enzymes in regulating transcription required for memory. *Learn. Mem.*, **15**, 460–467.
40. Korzus, E., Rosenfeld, M.G. and Mayford, M. (2004) CBP histone acetyltransferase activity is a critical component of memory consolidation. *Neuron*, **42**, 961–972.
41. Francis, Y.I., Fa, M., Ashraf, H., Zhang, H., Staniszewski, A., Latchman, D.S. and Arancio, O. (2009) Dysregulation of histone acetylation in the APP/PS1 mouse model of Alzheimer's disease. *J. Alzheimers Dis.*, **18**, 131–139.
42. Vecsey, C.G., Hawk, J.D., Lattal, K.M., Stein, J.M., Fabian, S.A., Attner, M.A., Cabrera, S.M., McDonough, C.B., Brindle, P.K., Abel, T. and Wood, M.A. (2007) Histone deacetylase inhibitors enhance memory and synaptic plasticity via CREB:CBP-dependent transcriptional activation. *J. Neurosci.*, **27**, 6128–6140.
43. Duff, K., Paulsen, J.S., Beglinger, L.J., Langbehn, D.R., Wang, C., Stout, J.C., Ross, C.A., Aylward, E., Carlozzi, N.E. and Queller, S. (2010) 'Frontal' behaviors before the diagnosis of Huntington's disease and their relationship to markers of disease progression: evidence of early lack of awareness. *J. Neuropsychiatry Clin. Neurosci.*, **22**, 196–207.
44. Ho, A.K., Sahakian, B.J., Brown, R.G., Barker, R.A., Hodges, J.R., Ane, M.N., Snowden, J., Thompson, J., Esmonde, T., Gentry, R., Moore, J.W. and Bodner, T. (2003) Profile of cognitive progression in early Huntington's disease. *Neurology*, **61**, 1702–1706.
45. Kirkwood, S.C., Siemers, E., Hodes, M.E., Conneally, P.M., Christian, J.C. and Foroud, T. (2000) Subtle changes among presymptomatic carriers of the Huntington's disease gene. *J. Neurol. Neurosurg. Psychiatry*, **69**, 773–779.
46. Kirkwood, S.C., Siemers, E., Bond, C., Conneally, P.M., Christian, J.C. and Foroud, T. (2000) Confirmation of subtle motor changes among presymptomatic carriers of the Huntington disease gene. *Arch. Neurol.*, **57**, 1040–1044.
47. Lemiere, J., Decruyenaere, M., Evers-Kiebooms, G., Vandenbussche, E. and Dom, R. (2004) Cognitive changes in patients with Huntington's disease (HD) and asymptomatic carriers of the HD mutation—a longitudinal follow-up study. *J. Neurol.*, **251**, 935–942.
48. Paulsen, J.S. (2009) Functional imaging in Huntington's disease. *Exp. Neurol.*, **216**, 272–277.
49. Rosas, H.D., Koroshetz, W.J., Chen, Y.I., Skeuse, C., Vangel, M., Cudkowicz, M.E., Caplan, K., Marek, K., Seidman, L.J., Makris, N., Jenkins, B.G. and Goldstein, J.M. (2003) Evidence for more widespread cerebral pathology in early HD: an MRI-based morphometric analysis. *Neurology*, **60**, 1615–1620.
50. Rosas, H.D., Salat, D.H., Lee, S.Y., Zaleta, A.K., Pappu, V., Fischl, B., Greve, D., Hevelone, N. and Hersch, S.M. (2008) Cerebral cortex and the clinical expression of Huntington's disease: complexity and heterogeneity. *Brain*, **131**, 1057–1068.
51. Wolf, R.C., Vasic, N., Schonfeldt-Lecuona, C., Ecker, D. and Landwehrmeyer, G.B. (2009) Cortical dysfunction in patients with Huntington's disease during working memory performance. *Hum. Brain Mapp.*, **30**, 327–339.
52. Brooks, S., Higgs, G., Jones, L. and Dunnett, S.B. (2010) Longitudinal analysis of the behavioural phenotype in Hdh((CAG)150) Huntington's disease knock-in mice. *Brain Res. Bull.*, doi:10.106/j.brainresbull.2010.05.004.
53. Murphy, K.P., Carter, R.J., Lione, L.A., Mangiarini, L., Mahal, A., Bates, G.P., Dunnett, S.B. and Morton, A.J. (2000) Abnormal synaptic plasticity and impaired spatial cognition in mice transgenic for exon 1 of the human Huntington's disease mutation. *J. Neurosci.*, **20**, 5115–5123.
54. Giralt, A., Saavedra, A., Carretón, O., Xifró, X., Alberch, J. and Pérez-Navarro, E. (2011) Increased PKA signaling disrupts recognition memory and spatial memory: role in Huntington's disease. *Hum. Mol. Genet.*, **20**, 4262–4247.
55. Won, J. and Silva, A.J. (2008) Molecular and cellular mechanisms of memory allocation in neuronetworks. *Neurobiol. Learn. Mem.*, **89**, 285–292.
56. Saura, C.A., Choi, S.Y., Beglopoulos, V., Malkani, S., Zhang, D., Shankaranarayana Rao, B.S., Chattarji, S., Kelleher, R.J III, Kandel, E.R., Duff, K., Kirkwood, A. and Shen, J. (2004) Loss of presenilin function causes impairments of memory and synaptic plasticity followed by age-dependent neurodegeneration. *Neuron*, **42**, 23–36.
57. Hardingham, G.E., Chawla, S., Cruzalegui, F.H. and Bading, H. (1999) Control of recruitment and transcription-activating function of CBP determines gene regulation by NMDA receptors and L-type calcium channels. *Neuron*, **22**, 789–798.
58. Wood, M.A., Attner, M.A., Oliveira, A.M., Brindle, P.K. and Abel, T. (2006) A transcription factor-binding domain of the coactivator CBP is essential for long-term memory and the expression of specific target genes. *Learn. Mem.*, **13**, 609–617.
59. Oike, Y., Hata, A., Mamiya, T., Kaname, T., Noda, Y., Suzuki, M., Yasue, H., Nabeshima, T., Araki, K. and Yamamura, K. (1999) Truncated CBP protein leads to classical Rubinstein-Taybi syndrome phenotypes in mice: implications for a dominant-negative mechanism. *Hum. Mol. Genet.*, **8**, 387–396.
60. Wood, M.A., Kaplan, M.P., Park, A., Blanchard, E.J., Oliveira, A.M., Lombardi, T.L. and Abel, T. (2005) Transgenic mice expressing a truncated form of CREB-binding protein (CBP) exhibit deficits in hippocampal synaptic plasticity and memory storage. *Learn. Mem.*, **12**, 111–119.
61. Caccamo, A., Maldonado, M.A., Bokov, A.F., Majumder, S. and Oddo, S. (2010) CBP gene transfer increases BDNF levels and ameliorates learning and memory deficits in a mouse model of Alzheimer's disease. *Proc. Natl Acad. Sci. USA*, **107**, 22687–22692.
62. Espana, J., Valero, J., Minano-Molina, A.J., Masgrau, R., Martin, E., Guardia-Laguarta, C., Lleo, A., Gimenez-Llort, L., Rodriguez-Alvarez, J. and Saura, C.A. (2010) beta-Amyloid disrupts activity-dependent gene transcription required for memory through the CREB coactivator CRTC1. *J. Neurosci.*, **30**, 9402–9410.
63. Fleischmann, A., Hvalby, O., Jensen, V., Strekalova, T., Zacher, C., Layer, L.E., Kvello, A., Reschke, M., Spanagel, R., Sprengel, R., Wagner, E.F. and Gass, P. (2003) Impaired long-term memory and NR2A-type NMDA receptor-dependent synaptic plasticity in mice lacking c-Fos in the CNS. *J. Neurosci.*, **23**, 9116–9122.
64. Guzowski, J.F. (2002) Insights into immediate-early gene function in hippocampal memory consolidation using antisense oligonucleotide and fluorescent imaging approaches. *Hippocampus*, **12**, 86–104.
65. Hallam, T.M. and Bourtchouladze, R. (2006) Rubinstein-Taybi syndrome: molecular findings and therapeutic approaches to improve cognitive dysfunction. *Cell Mol. Life Sci.*, **63**, 1725–1735.
66. Lagali, P.S., Corcoran, C.P. and Picketts, D.J. (2010) Hippocampus development and function: role of epigenetic factors and implications for cognitive disease. *Clin. Genet.*, **78**, 321–333.
67. Lockett, G.A., Wilkes, F. and Maleszka, R. (2010) Brain plasticity, memory and neurological disorders: an epigenetic perspective. *Neuroreport*, **21**, 909–913.

68. Tsankova, N., Renthal, W., Kumar, A. and Nestler, E.J. (2007) Epigenetic regulation in psychiatric disorders. *Nat. Rev. Neurosci.*, **8**, 355–367.
69. Levenson, J.M., O'Riordan, K.J., Brown, K.D., Trinh, M.A., Molfese, D.L. and Sweatt, J.D. (2004) Regulation of histone acetylation during memory formation in the hippocampus. *J. Biol. Chem.*, **279**, 40545–40559.
70. Levenson, J.M. and Sweatt, J.D. (2005) Epigenetic mechanisms in memory formation. *Nat. Rev. Neurosci.*, **6**, 108–118.
71. Stefanko, D.P., Barrett, R.M., Ly, A.R., Reolon, G.K. and Wood, M.A. (2009) Modulation of long-term memory for object recognition via HDAC inhibition. *Proc. Natl Acad. Sci. USA*, **106**, 9447–9452.
72. Rouaux, C., Loeffler, J.P. and Boutillier, A.L. (2004) Targeting CREB-binding protein (CBP) loss of function as a therapeutic strategy in neurological disorders. *Biochem. Pharmacol.*, **68**, 1157–1164.
73. Fischer, A., Sananbenesi, F., Wang, X., Dobbin, M. and Tsai, L.H. (2007) Recovery of learning and memory is associated with chromatin remodelling. *Nature*, **447**, 178–182.
74. Fischer, A., Sananbenesi, F., Mungenast, A. and Tsai, L.H. (2010) Targeting the correct HDAC(s) to treat cognitive disorders. *Trends Pharmacol. Sci.*, **31**, 605–617.
75. Kilgore, M., Miller, C.A., Fass, D.M., Hennig, K.M., Haggarty, S.J., Sweatt, J.D. and Rumbaugh, G. (2010) Inhibitors of class 1 histone deacetylases reverse contextual memory deficits in a mouse model of Alzheimer's disease. *Neuropsychopharmacology*, **35**, 870–880.
76. Ricobaraza, A., Cuadrado-Tejedor, M., Perez-Mediavilla, A., Frechilla, D., Del Rio, J. and Garcia-Osta, A. (2009) Phenylbutyrate ameliorates cognitive deficit and reduces tau pathology in an Alzheimer's disease mouse model. *Neuropsychopharmacology*, **34**, 1721–1732.
77. Ricobaraza, A., Cuadrado-Tejedor, M., Marco, S., Perez-Otano, I. and Garcia-Osta, A. (2010) Phenylbutyrate rescues dendritic spine loss associated with memory deficits in a mouse model of Alzheimer disease. *Hippocampus*, doi:10.1002/hipo.20883.
78. Bousiges, O., Vasconcelos, A.P., Neidl, R., Cosquer, B., Herbeaux, K., Panteleeva, I., Loeffler, J.P., Cassel, J.C. and Boutillier, A.L. (2010) Spatial memory consolidation is associated with induction of several lysine-acetyltransferase (histone acetyltransferase) expression levels and H2B/H4 acetylation-dependent transcriptional events in the rat hippocampus. *Neuropsychopharmacology*, **35**, 2521–2537.
79. Albasser, M.M., Poirier, G.L. and Aggleton, J.P. (2010) Qualitatively different modes of perirhinal-hippocampal engagement when rats explore novel vs. familiar objects as revealed by c-Fos imaging. *Eur. J. Neurosci.*, **31**, 134–147.
80. Guzowski, J.F., Lyford, G.L., Stevenson, G.D., Houston, F.P., McGaugh, J.L., Worley, P.F. and Barnes, C.A. (2000) Inhibition of activity-dependent arc protein expression in the rat hippocampus impairs the maintenance of long-term potentiation and the consolidation of long-term memory. *J. Neurosci.*, **20**, 3993–4001.
81. Labrousse, V.F., Costes, L., Aubert, A., Darnaudery, M., Ferreira, G., Amedee, T. and Laye, S. (2009) Impaired interleukin-1beta and c-Fos expression in the hippocampus is associated with a spatial memory deficit in P2X(7) receptor-deficient mice. *PLoS ONE*, **4**, e6006.
82. Fontan-Lozano, A., Romero-Granados, R., Troncoso, J., Munera, A., Delgado-Garcia, J.M. and Carrion, A.M. (2008) Histone deacetylase inhibitors improve learning consolidation in young and in KA-induced-neurodegeneration and SAMP-8-mutant mice. *Mol. Cell Neurosci.*, **39**, 193–201.
83. Ito, H., Yoshimura, N., Kurosawa, M., Ishii, S., Nukina, N. and Okazawa, H. (2009) Knock-down of PQBP1 impairs anxiety-related cognition in mouse. *Hum. Mol. Genet.*, **18**, 4239–4254.
84. Dompierre, J.P., Godin, J.D., Charrin, B.C., Cordelieres, F.P., King, S.J., Humbert, S. and Saudou, F. (2007) Histone deacetylase 6 inhibition compensates for the transport deficit in Huntingtoń s disease by increasing tubulin acetylation. *J. Neurosci.*, **27**, 3571–3583.
85. Ennaceur, A. and Delacour, J. (1988) A new one-trial test for neurobiological studies of memory in rats. 1: behavioral data. *Behav. Brain Res.*, **31**, 47–59.
86. Gines, S., Bosch, M., Marco, S., Gavalda, N., Diaz-Hernandez, M., Lucas, J.J., Canals, J.M. and Alberch, J. (2006) Reduced expression of the TrkB receptor in Huntington's disease mouse models and in human brain. *Eur. J. Neurosci.*, **23**, 649–658.